

**Translated from:** CAO Ge, CHENG Jie, BI Xiaobo, et al. Investigation on the numerical simulation of ship airwake based on DES [J]. Chinese Journal of Ship Research, 2016, 11(3): 48-54.

# Investigation on the numerical simulation of ship airwake based on DES

CAO Ge<sup>1,2</sup>, CHENG Jie<sup>1</sup>, BI Xiaobo<sup>1</sup>, ZHANG Zhiguo<sup>1</sup>, WANG Xianzhou<sup>1</sup>

1 School of Naval Architecture and Ocean Engineering, Huazhong University of Science and Technology, Wuhan 430074, China

2 Wuhan Military Representative Department, Naval Armament Department of PLAN, Wuhan 430074, China

**Abstract:** The superstructures of ships can generate different scales of vortices, a threat to the helicopter maneuvering. Aiming at the problem, the characteristics of the ship airwake is investigated in this paper with CFD method instead of the traditional Reynold-Averaged Navier-Stokes (RANS) method. In particular, Detached Eddy Simulation (DES) method is adopted to investigate the transitional flow field. Through processing the transitional data, a mean flow field is obtained, which agrees well with the experimental results, validating the effectiveness and accuracy of DES over RANS in solving ship airwake. Furthermore, by observing the transitional vortices, flow separation, and reattach of ship airwake with DES method, it is concluded that vortices' asymmetry is the main feature in wake flow, and the vortical magnitude sharply increases at the chimney, inducing a severe threat to the helicopter.

**Key words:** airwake; warship; Detached Eddy Simulation (DES); vortex

**CLC number:** U661.1

## 0 Introduction

The helicopter has become a critical part in modern naval combat actions, which has a very high tactical value. The superstructures of ships are made of a series of blunt bodies, which will generate different scales of vortices under ship moving or wind. When flow separates from hangar edge, shearing layer and slow-speed backflow region will be formed and lead to huge spatiotemporal velocity gradient in flow field of flight deck. Although the taking-off and landing of helicopter in ships have become a routine work, the highly unstable ship airwake is still the most dangerous environment that helicopter pilots face. The interaction between helicopter airscrew and vortices in airwake is the main reason of flight accident<sup>[1]</sup>, especially vortex flow and horizontal cross-flow area when the helicopter lands<sup>[2]</sup>. The interaction between downwash generated by helicopter main motor and

airwake makes the load of screw motor change and affects the engine power, causing difficulty for pilot's maneuvering<sup>[3]</sup>. In order to improve the security of helicopter, a large number of researches are carried out in many countries. TTCP (technology cooperation project) established by Australia, Canada, New Zealand, England and America commonly has funded many researches about ship airwake, and NATO reports also include many research reports about experiments and simulations of ship airwake.

Cheney and Zan et al.<sup>[4-5]</sup> measured average surface flow field of SFS model with scale ratio of 1:60 using film imaging method and used smog tracer method to achieve visualization of in vitro flow. On this basis, hot-wire anemometer was used to study the flow field of SFS2 model with scale ratio of 1:100 and the average speed and turbulence statistical values of a series of locations were measured along upper buildings and flight deck. In addition,

**Received:** 2015 - 06 - 10

**Author(s):** CAO Ge, male, born in 1983, engineer. Research interest: ship design and construction

CHENG Jie, male, born in 1990, Ph. D. candidate. Research interest: CFD and fluid dynamics. E-mail: chengj5@rpi.edu

ZHANG Zhiguo (Corresponding author), male, born in 1961, Ph. D., professor, Ph. D. supervisor. Research interest: CFD, fluid dynamics. E-mail: zzg@hust.edu.cn

the speed spectrum was also obtained.

In order to provide verification for the simulation calculation, Miklosovic et al.<sup>[6]</sup> performed wind tunnel test on the US patrol with the scale ratio of 1:25. Three heading angles 0°, 15° and 30° were selected in the experiment, Reynolds number was 7 600 000 and 18 hole probes were used to measure three-dimensional velocity field. The function of heading angle was considered to transform incoming flow into big vortex with the same magnitude as the superstructure. Besides, the instability of incoming flow was independent to the location of study plane under 0° heading angle, while the region where shear layers separate and rise forms a large vortex maximum band.

In low-speed wind tunnel, Mora<sup>[7]</sup> used Particle Image Velocimetry (PIV) system to carry out the research on the airwake of the frigate model's superstructure. Furthermore, the author used the acoustic velocimeter to measure the flow field of flight deck of the actual ship and compared it with that of wind tunnel experiment. Brownell et al.<sup>[8]</sup> measured the airwake of a navy training ship with the length of 108 ft, which provided verification data for CFD simulation. Polsky<sup>[9]</sup> used CFD method to perform real-time simulation on the unstable flow field generated by model under the function of 90° horizontal wind and found the grid quality was very critical to study this flow separation phenomenon.

Lu et al.<sup>[10-11]</sup> performed CFD numerical simulation on the airwake of the scale model of LHA-type ship and compared the LHA flow field results under different wind angles. According to research on SFS2 model by Gao and Liu<sup>[12]</sup>, the steady-state model not only satisfied the requirement of calculation precision, but reduced calculation time about this issue. By comparing the calculation results of several different turbulence models, the authors thought LK and MMK model were suitable. Chen et al.<sup>[13]</sup> used  $k-\omega$  model to carry out simulation calculation on airwake of a typical kind of ship and studied the movement law of gas flow and the vortex structure above the deck. Meanwhile, laser sheet light displaying system is used to measure the flow field in wind tunnel and verify the calculation result.

There were few researches on CFD simulation of ship airwake in China, most of which were steady-state simulation and used Reynold-Averaged Navier-Stokes (RANS) method<sup>[14]</sup>. As the most commonly used method in turbulence model, RANS method used statistical treatment of averaged flow

fluctuation as basis. Dependent variable is divided into an averaged part and the fluctuation component deviation of this averaged part. The equation of RANS is:

$$\partial_t \langle V \rangle + \nabla \cdot (\langle V \rangle \otimes \langle V \rangle) = -\nabla \langle p \rangle + \nabla \cdot (\langle S \rangle - R) \\ \nabla \cdot \langle V \rangle = 0$$

where  $\langle \rangle$  is the averaged part,  $R = \langle V' \otimes V' \rangle$  is the stress tensor of Reynold numbers, which describes the typical pulsation influence of averaged flow. For a statistically steady flow, the average value can be regarded as the average value in time. Although for the unsteady flow, the overall average value must be calculated, all turbulence flows are unstable and it is very difficult to predict whether the averaged flow description is precise enough to catch the basic flow characteristics. At the same time, it is impossible to obtain the detailed information of flow from its averaged flow.

Detached eddy simulation (DES) is a mixed RANS-LES method. In the region near wall, the scale of turbulence flow is very small, which can be calculated by RANS model. In separation region, the scale of turbulence flow is large and LES model was used for calculation after the scale more than the dimension of grid. Thus, DES is less precise than LES about the analysis of flow field, but better than RANS. Regarding the calculation amount, DES is between them. Based on the independent scale of fluid, DES can perform low-pass filtering and study the complex structure in the flow region, which is suitable for the simulation of aerodynamics. For the research on the flow field of ship airwake, DES can obtain the characteristic of flow field with time and also gain the averaged flow field information by averaging the transient flow field data with respect to time. This paper adopts DES to study the transient characteristic of ship airwake, reveal the turbulence feature of flow field and compare them with experimental data to verify the precision and effectiveness.

## 1 Basic theory of DES method

DES method includes Spalart-Allmaras model, Realizable  $k-\omega$  model and SST  $k-\omega$  model and so on. In DES simulation, the treatment of boundary layer uses unsteady-state RANS model, while separation region uses LES method. LES region is usually closely related to the core of turbulence, namely the region where large-scale and unstable turbulence plays important roles. In this region, DES is directly equal to LES model, while in the region near wall it

is equal to RANS model.

DES model is especially suitable to the wall flow with high Reynold number, which can be not calculated by LES in region near wall. However, in DES, RANS method can be used to solve this problem. When treating the outer flow field issue of aerodynamics with high Reynold number, DES model is a good choice. In DES model, the diffusion term of turbulence kinetic energy  $Y_k$  can be revised as<sup>[15]</sup>:

$$Y_k = \rho \beta^* k \omega F_{DES}$$

$$F_{DES} = \max\left(\frac{L_t}{C_{des} \Delta_{max}}, 1\right) \quad (1)$$

where  $\beta^*$  is a constant of SST model;  $\rho$  is density;  $k$  is the kinetic energy of turbulent fluctuation;  $\omega$  is energy dissipation rate;  $C_{des} = 0.61$ , which is the correction constant in DES model;  $\Delta_{max}$  is the local maximum grid gap ( $\Delta x, \Delta y, \Delta z$ );  $L_t$  is the parameter of turbulence scale in RANS model.

$$L_t = \frac{\sqrt{k}}{\beta^* \omega} \quad (2)$$

DES-SST model also provides the option (delay option) which "protects" boundary layer unconstrained.  $F_{DES}$  is corrected according to Eq. (3):

$$F_{DES} = \max\left(\frac{L_t}{C_{des} \Delta_{max}}(1 - F_{SST}), 1\right) \quad (3)$$

where  $F_{SST} = 0, F_1, F_2, F_1$  and  $F_2$  are the mixed functions of SST model.

## 2 Verification of CFD simulation

### 2.1 Simulation model and grid partition

This paper selects international general simulation model SFS2<sup>[16]</sup>, which is made of standard geometrical bodies. The heading is a triangular prism, the flight deck is located in stern, the ship length  $l = 455$  ft and width  $b = 45$  ft and the height of hanger  $h = 20$  ft. The geometrical representation is shown in Fig. 1, the  $x$  axis of coordinate system points to stern,  $y$  axis points to starboard and  $z$  axis straight up. The computational domain is cuboid, with a length of 9 times ship length, a width of 4.5 times ship length and a height of 0.75 times ship length. The issue of grid partition at bow can be solved by Y grid partition and the grid at bow is shown in Fig. 2.



Fig.1 Geometrical representation of SFS2 model



Fig.2 Y grid at bow

### 2.2 Grid independence verification

In order to verify grid independence, three different quantities  $G_i$  ( $i=1, 2, 3$ ) of grids are used and the number of nodes is 2 000 000, 6 780 000 and 8 200 000 respectively, which uses RANS for steady-state simulation. The simulation in this paper aims at isolated SFS2 model and the wind tunnel experimental data from Canada NRC<sup>[16]</sup> are cited to verify CFD simulation results (in order to be consistent with wind tunnel test, the model scale ratio is 1:100). The simulation adopts FLUENT pressure solver, with the second order interpolation format and the convective terms adopt three-order format. The boundary condition of ship body is no-slip wall surface, outlet is pressure-outlet, the velocity inlet is set as 1% of turbulence strength, the length scale is 0.304 8 m and other boundary conditions are set as no-friction wall surface.

A straight line parallel to  $y$  axis is selected at 50% of deck height and the height of hanger, whose length is twice the ship width. The velocity component  $V$  in  $x$  axis direction of each point in this line is recorded to compare with experimental data. Horizontal coordination adopts ship width  $b$  for non-dimension and the vertical coordination uses incoming velocity  $V_0$  infinite point for non-dimension. The result is shown in Fig. 3.

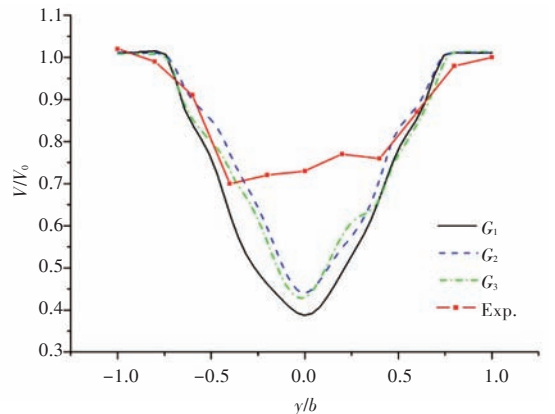


Fig.3 Grid independence evaluation at  $G_1, G_2$  and  $G_3$

When  $y/b$  is between  $-0.5 \sim 0.5$  (namely the width of flight deck), the simulation results of three grids

deviate much from experimental data. It is estimated that this place belongs to backflow region, the flow field is complex, which changes sharply under the influence of vortex, thus, RANS method cannot well predict the velocity, which indicates using the turbulence model more close to actual condition is necessary. By comparing the simulation results of three grids,  $G_2$  and  $G_3$  are close,  $G_1$  is much different from the two other. The grid in ship of  $G_2$  grid is 0.044 (using ship width for non-dimension), the flow field from flight deck to ship end is the research emphasis, grid is encrypted to 0.022. The grid along height from bottom plane to the highest point is 0.033, the grid height of the first layer in the boundary layer is 0.002, which guarantees that the value of  $y^+$  is in the range required by  $k-\varepsilon$  model. This shows  $G_2$  can be suitable for the simulation of air-wake flow field, thus,  $G_2$  grid is used in the further research.

From Fig.4 and Fig. 5, it can be clearly seen that the front edge which flows in the superstructure begins to separate and the strong shear occurs, which leads to the occurrence of vortex from downstream to hanger. From Fig.6 and Fig.7, a huge vortex structure is indeed formed at the 1/2 of the flight deck. From these, the flow separation at superstructure will reattach after through  $3h$  height. From Fig. 8, the backflow at the section of 1/2 deck length is three-dimensional, the velocity-weight along  $y$  direction also gathers from both sides to middle. The generation of backflow region brings difficulty to the prediction of flow field by steady-state simulation, thus the simulation results in Fig. 3 are all not close to the experimental values. On the other hand, the steady-state simulation results can not make us study the change of vortex structure in-depth, so, it is necessary to use high precision simulation.

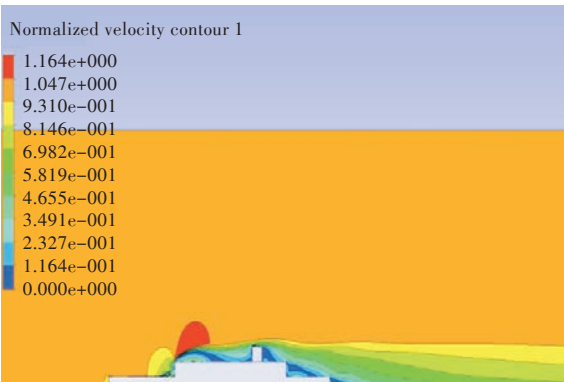


Fig.4 Velocity distribution at  $y=0$

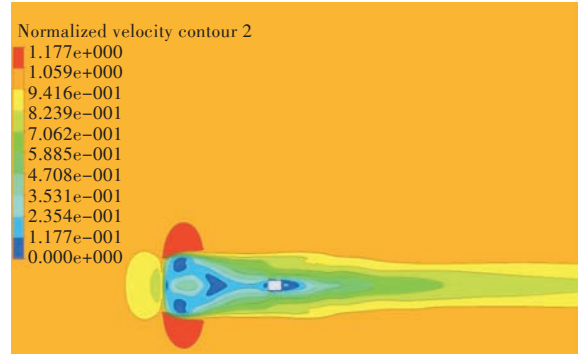


Fig.5 Velocity distribution at  $z=1.15h$

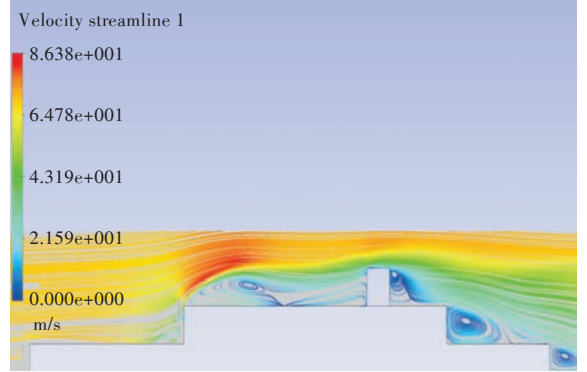


Fig.6 Streamline distribution colored by velocity at  $y=0$

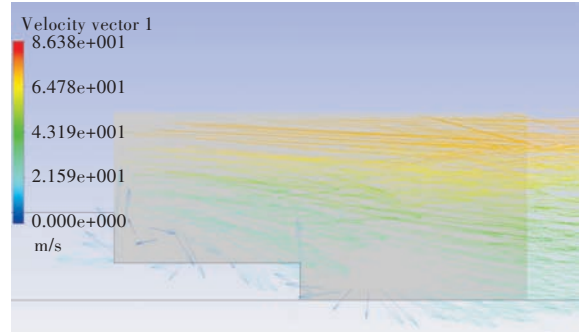


Fig.7 Velocity vector distribution at stern

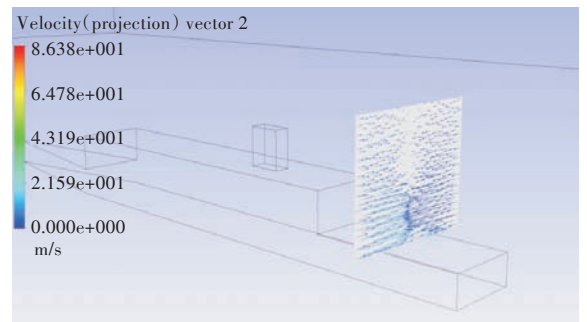


Fig.8 Velocity distribution in  $y$  direction at a certain section

## 3 Flow field simulation of ship air-wake based on DES

### 3.1 Mean flow field analysis

According to the recommended time step in Reference [15] and the simulation results in References

[17–18], time step with non-dimension selects  $d_t = 1.88 \times 10^{-2}$  (time step uses incoming velocity  $V_0$  and ship width  $b$  for non-dimension). Meanwhile, verification simulation is also conducted on  $d_t = 3.76 \times 10^{-2}$  and  $d_t = 9.4 \times 10^{-3}$ . It is found that the change of time step has little effect on simulation result, so simulation is based on reference value. After considering the effect of iteration times on results, the iteration times every time step is selected as 10. On the basis of steady-state simulation, after calculating 2 400 time steps, the flow field information is collected. Data are output each 4 steps, and the mean flow field information in DES is obtained by averaging of obtained data to time. Firstly, the velocity in the line of Section 2.2 is compared with experimental value, as shown in Fig. 9, where the horizontal coordinate is  $y/b$ , the vertical coordinate is the velocity with non-dimension. In order to compare with the simulation results of RANS, the velocity-weight by RANS is shown in Fig. 10.

By comparison of Fig. 9 and Fig. 10 ( $u, v, w$  represent  $x, y, z$  directions, respectively), it can be seen that DES evidently increases the precision of velocity along  $x$  and  $y$  directions. From Fig. 9, at the width from the deck edge to the center line, the velocity along  $x$  direction decreases evidently, which indicates this region encounters the airwake at the back of hanger. The same phenomenon also occurs in the velocity along  $z$  direction, which shows the separation flow at the top of hanger has the down feature. Although the weak asymmetry displayed in experimental data is not shown in CFD simulation, DES simulation results agree well with it in a whole, which indicates DES simulation is suitable for the ship airwake flow issue.

The six sections with width  $2b$ , height  $3h$  are selected at the 0%, 25%, 50%, 75%, 100% and 125%

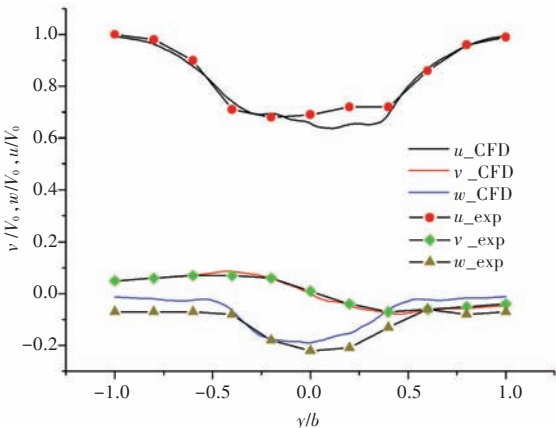


Fig.9 Mean velocity at different monitoring posts using DES

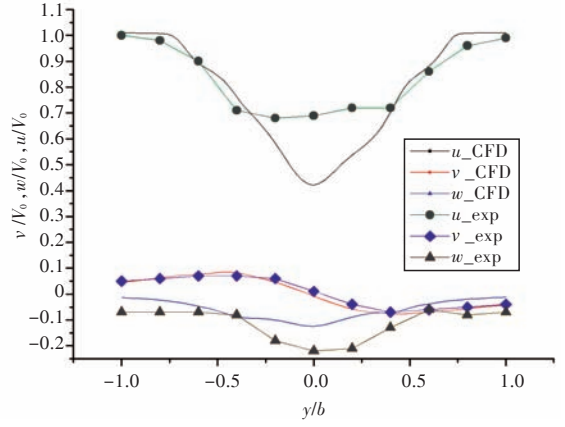


Fig.10 Mean velocity at different monitoring posts using RANS

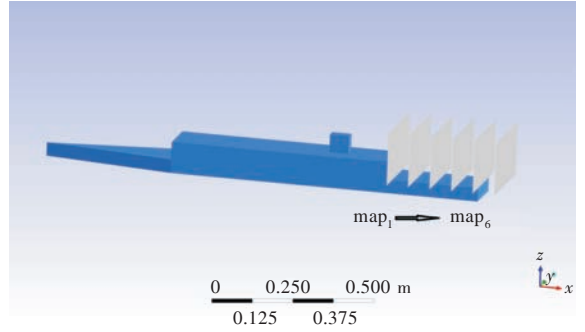


Fig.11 Sketch of map<sub>1</sub> to map<sub>6</sub>

of flight deck (Fig. 11), which are named as map<sub>1</sub> – map<sub>6</sub>, respectively. The distribution of mean velocity at each monitoring surfaces is shown in Fig. 12. From Fig. 12, after sampling 600 time points, the mean flow field calculated by DES can reflect the whole feature of flow field and the flow field displays better symmetry. Back from the flight deck, the influence of superstructure on flow field becomes weak gradually, after 75%, only the velocity near deck decreases slightly.

### 3.2 Instantaneous flow field analysis

Based on the DES instantaneous analysis, the instantaneous non-dimensional velocity contours at  $y=0$  and  $z=1.15h$  are shown in Fig. 13. From the figure, instantaneous flow field can reflect the irregular characteristic of turbulence field.

Next, the core region of vortex is judged according to the method in Reference [19]. The criterion of judgment is  $\lambda_2$ .  $\lambda_2$  is the second feature value of  $S^2 + \Omega^2$ ,  $S$  and  $\Omega$  are the symmetric part and asymmetric part of velocity tensor.  $\lambda_2 < 0$  indicates the occurrence of vortex core in this place, the smaller  $\lambda_2$  is, the stronger the vortex is. The instantaneous  $\lambda_2$  distribution at two sections is shown in Fig. 14. Fig. 15 shows the section of  $\lambda_2 = 0$ , which displays the vortex core of ship hull surface. From

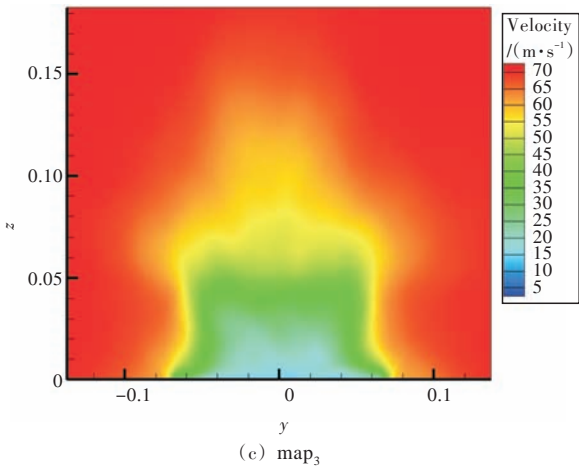
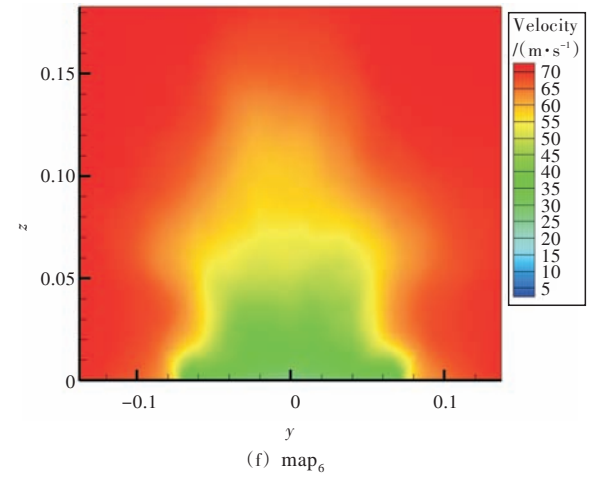
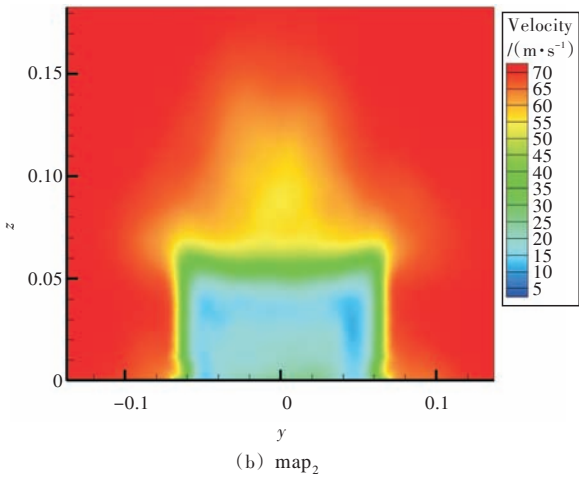
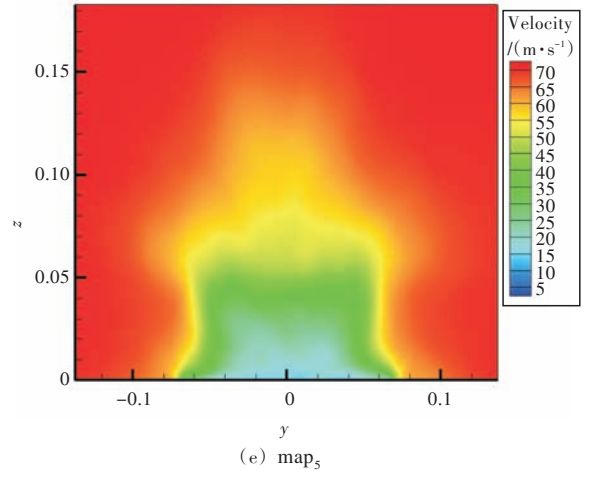
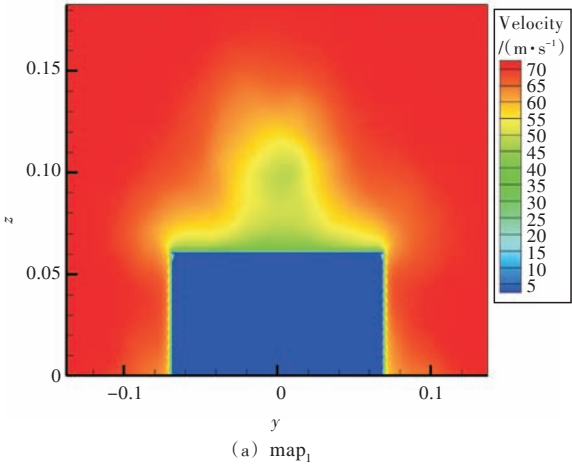


Fig.12 Distribution of mean velocity at different monitoring surfaces

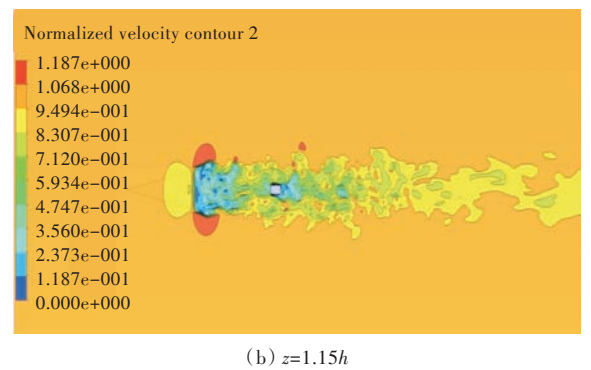
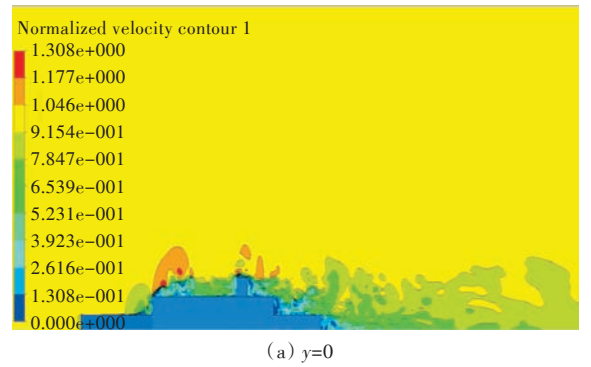
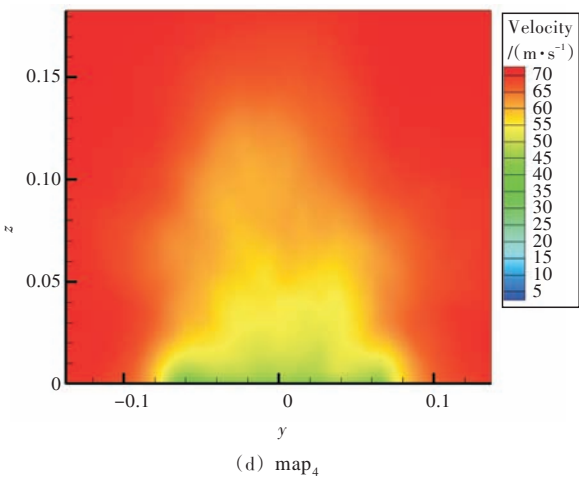


Fig.13 Instantaneous non-dimensional velocity contours at  $y=0$  and  $z=1.15h$ , respectively

Figures, after flow separates, a series of vortices are formed and display asymmetry. From upstream to downstream, the strength of vortex decreases gradually, but after encountering chimney, the strength of vortex increases sharply. When helicopter hovers at the chimney height of flight deck, the vortices falling out of chimney may be harmful to it. Flow gathers from the left, right and upper to middle in flight deck and forms a three-dimensional bubble in the back-end of hanger, which decreases the strength of the latter vortices. In a whole, the main feature of instantaneous flow field is asymmetry and vortex structure.

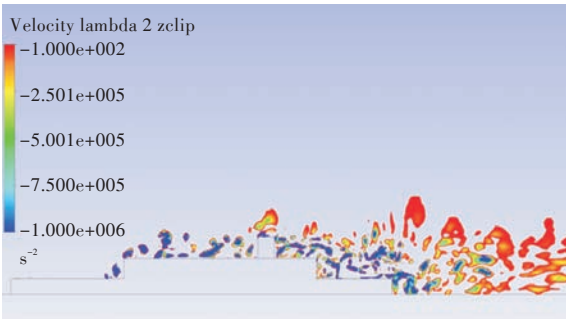
results indicate that:

1) DES is suitable for the simulation of ship airwake, the simulation results well agree with experimental data, which can more accurately predict the flow field at the back of hanger compared with RANS.

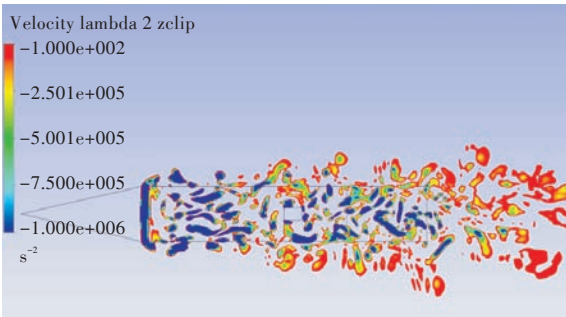
2) Vortex structure and asymmetry are the main features of ship airwake, flow reattaches at about  $3h$  of flight deck, while the strength of vortex increases sharply at the chimney, which may be harmful to the helicopter maneuvering.

## References

- [1] HEALEY J V. The aerodynamics of ship superstructures [C]//Neuilly Surseine: Proceedings of AGARD Conference–Aircraft Ship Operations, 1991: 1–14.
- [2] AZUMA A, SAITO S, KAWACHI K. Response of a helicopter penetrating the tip vortices of a large airplane [J]. *Vertica*, 1987, 11(1/2): 65–76.
- [3] REDDY R, TRUONG T. Effect of ship airwake interference on helicopter trim and control positions [C]// Proceedings of the 12th Australasian Fluid Mechanics Conference. Australia: The University Sydney, 1995: 691–696.
- [4] CHENEY B T, ZAN S J. CFD code validation data and flow topology for the technical co-operation program AER-TP2 simple frigate shape [R]. Canada: National Research Council, 1999.
- [5] ZAN S J. Surface flow topology for a simple frigate shape [J]. *Canadian Aeronautics and Space Journal*, 2001, 47(1): 33–43.
- [6] MIKLOSOVIC D S, KANG H S, SNYDER M R. Ship air wake wind tunnel test results [C]// 29th AIAA Applied Aerodynamics Conference. San Francisco: AIAA, 2011: 27–30.
- [7] MORA R B. Flow field velocity on the flight deck of a frigate [J]. *Proceedings of the Institution of Mechanical Engineers Part G–Journal of Aerospace Engineering*, 2014, 228(14): 2674.
- [8] BROWNELL C J, LUZNIKL L, SNYDER M R, et al. In situ velocity measurements in the near-wake of a ship superstructure [J]. *Journal of Aircraft*, 2012, 49(5): 1440–1450.
- [9] POLSKY S A. CFD prediction of airwake flowfields for ships experiencing beam winds [C]//21st AIAA Applied Aerodynamics Conference. Orlando, Florida: AIAA, 2003: 23–26.
- [10] LU Chao, JIANG Zhifang, WANG Tao. Influences of different airflow situations for ship airwake [J]. *Ship Science and Technology*, 2009, 31(9): 38–42 (in



(a)  $y=0$



(b)  $z=1.15h$

Fig.14 Instantaneous  $\lambda_2$  distribution at  $y=0$  and  $z=1.15h$ , respectively

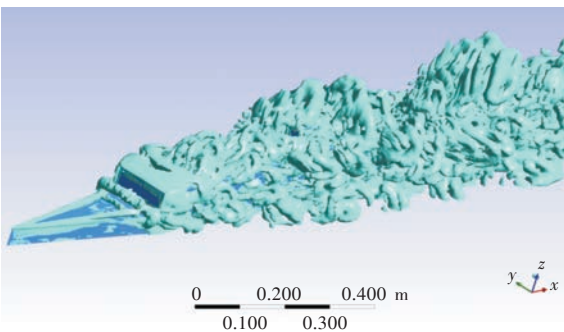


Fig.15 Structure of vortex core ( $\lambda_2 = 0$ )

## 4 Conclusions

Based on DES, this paper performs numerical simulation on the ship airwake and compares with experimental research results. The numerical simulation

- Chinese).
- [11] LU Chao, JIANG Zhifang, WANG Tao. Simplified evaluation of ship airwake characteristics for takeoff/landing of shipborne aircraft [J]. Chinese Journal of Ship Research, 2010, 5(1): 39-42(in Chinese).
- [12] GAO Ye, LIU Changmeng. Numerical calculation of frigate ship airwake [J]. Journal of Harbin Engineering University, 2013, 34(5): 599-603(in Chinese).
- [13] CHEN Jixiang, ZHU Xucheng, WANG Qiang, et al. Analysis of the characteristics of typical ship's airwake [J]. Journal of Naval Aeronautical Engineering Institute, 2012, 27(5): 517-520, 524(in Chinese).
- [14] POPE S B. Turbulent flows [M]. Cambridge: Cambridge University Press, 2000.
- [15] SPALART P R. Guide to detached-eddy simulation grids: NASA/CR -2001-211032 [R]. 2001.
- [16] KIM J M, KOMERATH N M. Summary of the interaction of a rotor wake with a circular cylinder[J]. AIAA Journal, 1995, 33(3): 470-478.
- [17] HEDGES L S, TRAVIN A K, SPALART P R. Detached-eddy simulations over a simplified landing gear [J]. Journal of Fluids Engineering, 2002, 124(2): 413-423.
- [18] FORSYTHE J R, SQUIRES K D, WURTZLER K E, et al. Detached-eddy simulation of the F-15E at high alpha[J]. Journal of Aircraft, 2004, 41(2): 193-200.
- [19] JEONG J, HUSSAIN F. On the identification of a vortex [J]. Journal of Fluid Mechanics, 1995, 285: 69-94.

## 基于DES的舰船空气尾流场特性分析

操戈<sup>1,2</sup>, 程捷<sup>1</sup>, 毕晓波<sup>1</sup>, 张志国<sup>1</sup>, 王先洲<sup>1</sup>

1 华中科技大学 船舶与海洋工程学院, 湖北 武汉 430074

2 海军装备部 驻武汉地区军事代表局, 湖北 武汉 430064

**摘要:** 舰船上层建筑后方产生湍流尾流场会对舰载直升机的操纵产生严重威胁。采用CFD方法对舰船空气尾流场的特性进行分析研究,突破了雷诺时均方法的局限性,使用分离涡模拟(DES)方法求解瞬态舰船尾流场,按照一定频率采样流场数据,得出的平均流场明显比RANS方法的结果更贴近实验数据,证明了此方法的有效性。同时,运用DES方法直观地观察尾流场的涡特性、流动分离和再附着等特征,发现涡结构及其不对称性是舰船空气尾流场的主要特征,涡强度在烟囱处突然增强,可能对直升机的操纵产生不利影响。

**关键词:** 空气尾流; 舰船; 分离涡模拟(DES); 涡